doi:10.1093/brain/awq135 Brain 2010: 133; 1930–1943 | 1930

BRAIN
A JOURNAL OF NEUROLOGY

Nicotinic acid adenine dinucleotide phosphate-mediated calcium signalling in effector T cells regulates autoimmunity of the central nervous system

Chiara Cordiglieri,[1,*,†] Francesca Odoardi,[1,2,3,†] Bo Zhang,[4] Merle Nebel,[5] Naoto Kawakami,[1] Wolfgang E. F. Klinkert,[1] Dimtri Lodygin,[2] Fred Lühder,[2] Esther Breunig,[6] Detlev Schild,[6] Vijay Kumar Ulaganathan,[1] Klaus Dornmair,[1,7] Werner Dammermann,[5] Barry V. L. Potter,[4,†] Andreas H. Guse[5,†] and Alexander Flügel[1,2,3,†]

1 Department of Neuroimmunology, Max-Planck-Institute for Neurobiology, 82152 Martinsried, Germany
2 Department Neuroimmunology, Institute for Multiple-Sclerosis-Research, University of Göttingen and Hertie Foundation, 37073 Göttingen, Germany
3 Institute for Immunology, Ludwig Maximilians University, 80336 Munich, Germany
4 Wolfson Laboratory of Medicinal Chemistry, Department of Pharmacy and Pharmacology, University of Bath, Bath, BA2 7AY, UK
5 The Calcium Signalling Group, Centre of Experimental Medicine, Institute of Biochemistry and Molecular Biology I: Cellular Signal Transduction, University Medical Centre Hamburg-Eppendorf, 20246 Hamburg, Germany
6 Department of Neurophysiology and Cellular Biophysic, University of Göttingen, 37083 Göttingen, Germany
7 Institute for Clinical Neuroimmunology, Ludwig-Maximilians-University, 81377 Munich, Germany

*Present address: Department of Neuroimmunology and Neuromuscolar Disorders, Istituto Neurologico Carlo Besta, 20133 Milano, Italy.
†These authors contributed equally to this work.

Correspondence to: Alexander Flügel,
Institute for Multiple-Sclerosis-Research,
Department of Neuroimmunology,
University of Göttingen, Waldweg 33,
37073 Göttingen, Germany
E-mail: fluegel@neuro.mpg.de

Nicotinic acid adenine dinucleotide phosphate represents a newly identified second messenger in T cells involved in antigen receptor-mediated calcium signalling. Its function *in vivo* is, however, unknown due to the lack of biocompatible inhibitors. Using a recently developed inhibitor, we explored the role of nicotinic acid adenine dinucleotide phosphate in autoreactive effector T cells during experimental autoimmune encephalomyelitis, the animal model for multiple sclerosis. We provide *in vitro* and *in vivo* evidence that calcium signalling controlled by nicotinic acid adenine dinucleotide phosphate is relevant for the pathogenic potential of autoimmune effector T cells. Live two photon imaging and molecular analyses revealed that nicotinic acid adenine dinucleotide phosphate signalling regulates T cell motility and re-activation upon arrival in the nervous tissues. Treatment with the nicotinic acid adenine dinucleotide phosphate inhibitor significantly reduced both the number of stable arrests of effector T cells and their invasive capacity. The levels of pro-inflammatory cytokines interferon-gamma and interleukin-17 were strongly diminished. Consecutively, the clinical symptoms of experimental autoimmune encephalomyelitis were ameliorated. *In vitro*, antigen-triggered T cell proliferation and cytokine production were evenly suppressed. These inhibitory effects were reversible: after wash-out of the nicotinic acid adenine dinucleotide phosphate antagonist, the effector T cells fully regained their functions. The nicotinic acid derivative BZ194 induced this transient state of non-responsiveness specifically in

Received October 16, 2009. Revised April 23, 2010. Accepted April 25, 2010. Advance Access publication June 2, 2010
© The Author(s) 2010. Published by Oxford University Press on behalf of Brain.
This is an Open Access article distributed under the terms of the Creative Commons Attribution Non-Commercial License (http://creativecommons.org/licenses/by-nc/2.5), which permits unrestricted non-commercial use, distribution, and reproduction in any medium, provided the original work is properly cited.

post-activated effector T cells. Naïve and long-lived memory T cells, which express lower levels of the putative nicotinic acid adenine dinucleotide phosphate receptor, type 1 ryanodine receptor, were not targeted. T cell priming and recall responses *in vivo* were not reduced. These data indicate that the nicotinic acid adenine dinucleotide phosphate/calcium signalling pathway is essential for the recruitment and the activation of autoaggressive effector T cells within their target organ. Interference with this signalling pathway suppresses the formation of autoimmune inflammatory lesions and thus might qualify as a novel strategy for the treatment of T cell mediated autoimmune diseases.

Keywords: experimental autoimmune encephalomyelitis; multiple sclerosis; T cell signalling; nicotinic acid adenine dinucleotide phosphate; intravital imaging

Abbreviations: DMSO = dimethyl sulphoxide; GFP = green fluorescent protein; (^{3}H)dT = (^{3}H)-2′-deoxy-thymidine; IFN-γ = interferon-gamma; IP_3 = D-*myo*-inositol 1,4,5-trisphosphate; MBP = myelin basic protein; NAADP = nicotinic acid adenine dinucleotide phosphate; OVA = ovalbumin; EAE = experimental autoimmune encephalomyelitis.

Introduction

Elevation of the free cytosolic and nuclear Ca^{2+} concentration is an essential event during T cell activation and is controlled by a complex network of different molecules. The major source of Ca^{2+} is the extracellular space. Ca^{2+} entry from this extracellular source is guided by the recently discovered Ca^{2+} channels Orai1/Ca^{2+} release-activated Ca^{2+} channel membrane protein 1 (CRACM1) (Feske *et al.*, 2006; Peinelt *et al.*, 2006; Vig *et al.*, 2006; Yeromin *et al.*, 2006). The opening of these channels, however, requires continuous Ca^{2+} release from intracellular pools. The best known Ca^{2+} mobilizing second messenger is D-*myo*-inositol 1,4,5-trisphosphate (IP_3) (Streb *et al.*, 1983), but two additional molecules, cyclic ADP-ribose (Guse *et al.*, 1999) and nicotinic acid adenine dinucleotide phosphate (NAADP) (Berg *et al.*, 2000), were found to release Ca^{2+} from the intracellular pool of T cells. Recent work in Jurkat lymphoma cells indicates that a timely coordinated release and interplay of these three messengers is required in shaping the Ca^{2+} signal after T cell receptor-triggered antigen stimulation (Guse *et al.*, 1999; Gasser *et al.*, 2006).

Due to a lack of biocompatible and specific inhibitors, the functional impact of each distinct Ca^{2+}-mobilizing second messenger following antigen-driven activation is less well understood. Recently, we developed an antagonist, BZ194, which interferes selectively with NAADP-mediated Ca^{2+} release via the type 1 ryanodine receptor in T cells. Initial *in vitro* analyses of the functional consequences of NAADP antagonism revealed that BZ194 efficiently suppressed T cellular interleukin-2 production and proliferation (Dammermann *et al.*, 2009).

Since effector T cells reactive against self-antigens are thought to cause organ-specific autoimmune diseases (Steinman *et al.*, 1995), we investigated here the therapeutic potential of BZ194 in experimental autoimmune encephalomyelitis (EAE), the classic T cell mediated animal model for multiple sclerosis (Wekerle *et al.*, 1994). We genetically labelled the effector T cell population to track the disease-inducing cell populations upon NAADP inhibition *in vivo* (Flügel *et al.*, 1999). Our data demonstrate that NAADP-driven reactivation of autoaggressive effector T cells within their target organs plays an essential role in the induction of autoimmune diseases of the nervous system.

Materials and methods

Materials

Fura-2/AM was purchased from Calbiochem. NAADP and dimethyl sulphoxide (DMSO) were supplied by Sigma. BZ194 was synthesized as described (Dammermann *et al.*, 2009).

Animals

Lewis and DA rats were obtained from the animal breeding facilities of the Max Planck Institute for Biochemistry (Martinsried, Germany) and kept under standardized conditions. All experiments were conducted according to Bavarian state regulations for animal experimentation and approved by the responsible authorities.

Generation and culture of effector T cells

Antigen-specific effector T cell clones were obtained from lymph node preparations of immunized Lewis rats. Stimulation, expansion and culture of specific rat T cells were conducted as described (Flügel *et al.*, 1999). Details concerning generation of myelin basic protein (MBP)- and ovalbumin (OVA)-specific $CD4^+$ T cells (T_{MBP} and T_{OVA}–cells) retrovirally engineered to express the marker gene *EGFP* are provided in the Supplementary Methods section.

Proliferation assays of T cells

Antigen-specific rat T cells (T_{MBP} and T_{OVA} cells) were co-cultured for 48 h in 96-well plates (in Dulbecco's modified Eagle's medium 1% rat serum) with irradiated professional thymic antigen presenting cells as previously described (Flügel *et al.*, 1999), in presence of specific or control antigen (10 µg/ml MBP or OVA) and BZ194 in DMSO, or DMSO alone. Amplification of $T_{MBP\text{-}GFP}$ cells was measured either by cytofluorometry or by (^{3}H)-2′-deoxy-thymidine [(^{3}H)dT; 2 Ci/mmol; Amersham] incorporation. Further details are included in the Supplementary Methods section. To rule out that BZ194 treatment interferes with the T cell proliferation machinery, T_{MBP} cell blasts 2 days following stimulation with MBP-pulsed professional antigen presenting cells were incubated with increasing amounts of BZ194 and their numbers determined 24, 48 and 96 h later by cytofluorometry. After removal of BZ194 the T cells were then re-stimulated with

MBP-pulsed antigen presenting cells. (^{3}H)dT incorporation was used to evaluate proliferation after 2 days culture.

To test antigen reactivity of BZ194-treated T cells, the cells were first stimulated with MBP-pulsed antigen presenting cells in the presence of increasing amounts of BZ194 for 48 h, or in the presence of vehicle alone (DMSO, vehicle). Thereafter, the cells were rechallenged with MBP-pulsed antigen presenting cells and their proliferation rate was evaluated 2 days later by (^{3}H)dT incorporation. For stimulation of effector and naïve T cells by anti-CD3/anti-CD28 antibodies (Serotec), 96-well plates were coated for 2 h at room temperature with 5 μg/ml of each antibody in phosphate buffered saline. Rat T_{MBP} and T_{OVA} effector cells or OX 22^{high} (CD45-RC$^+$) naïve T cells were plated at the final concentration of 10^5 cells/well. After Day 2 of culturing, (^{3}H)dT incorporation was measured. Naive CD45-RC$^+$ T cells (Powrie and Mason, 1988; Ramirez and Mason, 2000) were isolated from lymph nodes of untreated animals using fluorescence activated cell sorting (FACS Vantage, Becton Dickinson).

Memory T cells were prepared as described (Kawakami *et al.*, 2005*b*). More information is provided in the Supplementary Methods section.

EAE and BZ194 application *in vivo*

For induction of transfer EAE, 5×10^6 MBP-reactive GFP$^+$ T cells were injected i.v. into healthy recipient rats. Active EAE was induced by intra-cutaneous injection of 100 μg MBP emulsified in complete Freund's adjuvant containing *Mycobacterium tuberculosis* (4 mg/ml; DIFCO). Animals were monitored daily by measuring weight and examining disease scores as follows: 0 = no disease; 1 = flaccid tail; 2 = gait disturbance; 3 = complete hind limb paralysis; 4 = tetraparesis; 5 = death. The observation time was extended to more than 30 days during active EAE and 21 days during adoptive transfer EAE.

For treatment, daily i.p. injections of BZ194 (500 μM, 180 mg/kg, solubilized in DMSO/1% Lewis rat serum), DMSO (0.8 ml/kg) or nicotinic acid (500 μM, 61.5 mg/kg, solubilized in DMSO/1% Lewis rat serum) were performed. Application of BZ194 in concentrations of up to 1 mM for 7 days or 0.5 mM for 14 days did not show any overt toxic effect. Treatment with 180 mg/kg BZ194 per day was chosen since this dose resulted in serum levels of ~300 μM, as determined by a T cell proliferation bioassay (Supplementary Fig. 12; Supplementary Methods section). This concentration was sufficient to suppress proliferation of T_{MBP} effector cells (Fig. 3A and B, 5A).

Antigen presentation capacity of BZ194-treated lymph node cells

Lymph node cells from BZ194- or DMSO-treated animals were harvested and irradiated (5000 rad). Resting T_{MBP} or T_{OVA} cells were then added to the cultures and proliferation in the presence of specific or control antigen (10 μg/ml MBP or OVA, respectively) was determined by (^{3}H)dT incorporation 2 days later.

Mylein basic protein-reactive antibody production after BZ194 treatment of myelin basic protein immunized animals

Vinyl plates (96-well) (Corning-Costar) were coated with MBP (10 μg/ml) for 1 h at 37°C in a buffer containing 0.025 M Na_2CO_3 and 0.025 M $NaHCO_3$. Blood samples were taken 0, 7 and 14 days after immunization. Detection of MBP-specific antibodies was performed via enzyme-linked immunosorbent assay on different serum dilutions (1:500, 1:1000 and 1:2000). More information is provided in the Supplementary Methods section.

Quantitative polymerase chain reaction and enzyme-linked immunosorbent assays

Detailed information is provided in the Supplementary Methods section.

Cell isolation, cytofluorometry, fluorescence-activated cell sorting and immunohistochemistry

Single cell suspensions from organs were prepared as described previously (Flügel *et al.*, 2001). Detailed information is provided in the Supplementary Methods section.

Chemotaxis assays

Ex vivo isolated or *in vitro* cultured effector T cells were tested for their ability to pass through a 5 μm pore membrane following a chemokine gradient by using transwell plates (Corning-Costar). Detailed information is provided in the Supplementary Methods section.

Lipopolysaccharide-induced central nervous system inflammtion

Lipopolysaccharide (150 ng) from *Escherichia coli* 0127:B8 (Sigma) in a volume of 25 μl or an equivalent volume of phosphate buffered saline was intrathecally injected into the cisterna magna of anaesthetized animals.

Live imaging

Preparation of acute spinal cord slices and live imaging were performed as described (Kawakami *et al.*, 2005*b*; Bartholomäus *et al.*, 2009). Detailed information is provided in the Supplementary Methods section.

Statistical analysis

For statistical evaluation a two-tailed *t*-test with homeostatic variance was used in all assays except clinical evaluation of EAE, where the Mann–Whitney U-ranking test was applied using the MedCalc software (http://www.medcalc.be).

Results

NAADP antagonist BZ194 ameliorates experimental autoimmune encephalomyelitis

The role of NAADP signalling in T cell-mediated autoimmune diseases was tested using BZ194 (Supplementary Fig. 1), a lipophilic derivative of the nicotinic acid group of the molecule

(Dammermann *et al*., 2009). Healthy animals tolerated the NAADP antagonist (12 days, 180 mg/kg i.p.) without any apparent adverse effect. The size and the cellularity of primary and secondary lymph organs and the blood were not altered (Supplementary Fig. 2A). The reactivity of the lymph node cells, as tested in mixed lymphocyte reactions (Supplementary Fig. 2B) and the antigen presenting capacity of *ex vivo* isolated antigen presenting cells remained unaffected (Supplementary Fig. 2C).

The incidence and severity of clinical EAE induced by active immunization with MBP was significantly reduced by BZ194 (Fig. 1A; Table 1). This was accompanied by a decreased inflammation of the spinal cord, the preferentially affected CNS location in this EAE model (Supplementary Fig. 3A–C). Notably, BZ194 injection immediately before onset of the clinical disease, i.e. in the 'effector' phase of EAE, was similarly effective as when 'preventively' applied, i.e. during the 'priming' phase of EAE, simultaneously with immunization (Fig. 1B, Table 1). Active EAE evolves in two phases: during the initial disease-free phase, naïve T cells carrying the appropriate antigen-receptor become activated within the draining lymph nodes upon encounter of the applied brain antigen presented by professional antigen presenting cells. In the second phase, the 'primed' cells then migrate as effector T cells into the CNS where they re-encounter endogenous brain antigen presented by local antigen presenting cells. The ensuing re-activation and cytokine production of the autoaggressive effector T cells initiate and drive CNS inflammation and paralytic disease (Kawakami *et al*., 2004).

Obviously, BZ194 did not impair the stimulation of naïve T cells during the primary immune responses after immunization: T cell proliferation within draining lymph nodes, pro-inflammatory cytokine production and MBP-specific antibody responses were not changed (Fig. 1C–E).

NAADP antagonist BZ194 induces a transient state of non-responsiveness to antigen stimulation of (auto)antigen experienced effector T cells

These observations led us to explore the effects of BZ194 on post-activated effector T cells. To this end, we generated MBP-specific $CD4^+$ T cell lines (Ben-Nun *et al*., 1981). The NAADP antagonist significantly reduced Ca^{2+} signalling (Supplementary Fig. 4A), proliferation (Fig. 2A) and the production of interleukin-2 upon antigen receptor-triggered stimulation (Dammermann *et al*., 2009). Additionally, the levels of the pro-inflammatory cytokines interferon-gamma (IFN-γ) and interleukin-17 were significantly reduced (Supplementary Fig. 4B and C). The expression of interleukin-4 remained barely detectable, the levels of interleukin-10, TNFα and the chemokine receptors C-X-C chemokine receptor type 3 (CXCR3) and C-C chemokine receptor type 5 (CCR5) were not significantly changed. The early growth response genes 2 and 3 (*egr2* and *egr3*) were strongly up-regulated (Supplementary Fig. 4D).

Notably, the effect of BZ194 was reversible: after wash-out of BZ194 the effector T cells regained responsivity to their antigen. Re-challenge with antigen-pulsed antigen presenting cells after wash-out of BZ194 completely restored proliferation and cytokine production of the T cells (scheme in Fig. 2A and B; Supplementary Fig. 4E). BZ194 was efficient when applied before the T cells came in contact with antigen-pulsed antigen presenting cells. This is most likely due to the fact that NAADP-mediated Ca^{2+} fluxes occur early during T cell activation (Gasser *et al*., 2006). Accordingly, BZ194 did not impair T cell proliferation when it was applied after this early stimulation phase, i.e. 48 h after co-cultivation with antigen presenting cells (scheme in Fig. 2C and D). Even upon prolonged BZ194 exposure (up to 96 h) after wash-out, the effector T cells grew indistinguishably from untreated cells when specifically stimulated with MBP (Fig. 2D). The suppressive effects of BZ194 were not due to interference with the function of antigen presenting cells, since T cell proliferation was efficiently inhibited by BZ194 after stimulating the cells in the absence of antigen presenting cells using anti-CD3 and anti-CD28 antibodies (Fig. 3A and B). Furthermore, pretreatment of antigen presenting cells with BZ194 for 2 and 16 h did not change their capacity to stimulate effector MBP- or OVA-specific T cells (Supplementary Fig. 5).

Naïve and memory T cells are less susceptible to NAADP antagonism

Remarkably, we observed a clear difference between the inhibitory potency of BZ194 for antigen-experienced effector T cells and OX 22^{high} ($CD45\text{-}RC^+$) naïve T cells, i.e. T cells that had not been confronted with antigen before (Powrie and Mason, 1988, Ramirez and Mason, 2000). While the proliferation of cultured (Fig. 3A) or *ex vivo*-isolated (Supplementary Fig. 6A) antigen-experienced effector T cells was inhibited starting at a concentration of ~50 μM BZ194, naïve cells responded to the treatment only at more than 10-fold higher concentrations ($\geqslant$750 μM, Fig. 3A). Reduced sensitivity to BZ194 was also detected in long-lived memory T cells.

The proliferation of OVA-reactive memory T_{GFP} cells that had been instilled into neonatal animals and that had persisted for 6 months as classical resting memory T cells (Kawakami *et al*., 2005*b*) was suppressed starting at $\geqslant$500 μM BZ194 (Fig. 3B). Similar data were obtained with human naive and memory T cell responses (Supplementary Fig. 6B). The differential susceptibility to BZ194 correlated with the expression of ryanodine receptor 1, which was recently identified as the putative receptor for NAADP-triggered Ca^{2+} signalling in T cells (Dammermann *et al*., 2009). Ryanodine receptor 1 was significantly up-regulated in effector T cells as compared to naïve and memory T cells (Fig. 3C).

NAADP antagonism interferes with re-activation of autoaggressive effector T cells within their target organ

We next explored the effects of NAADP antagonist BZ194 on autoaggressive effector T cells *in vivo*. For this purpose we induced EAE by transfer of activated effector T_{MBP} cells that were retrovirally engineered to express green fluorescent protein (GFP) as genetic marker (effector $T_{MBP\text{-}GFP}$ cells) (Flügel *et al*.,

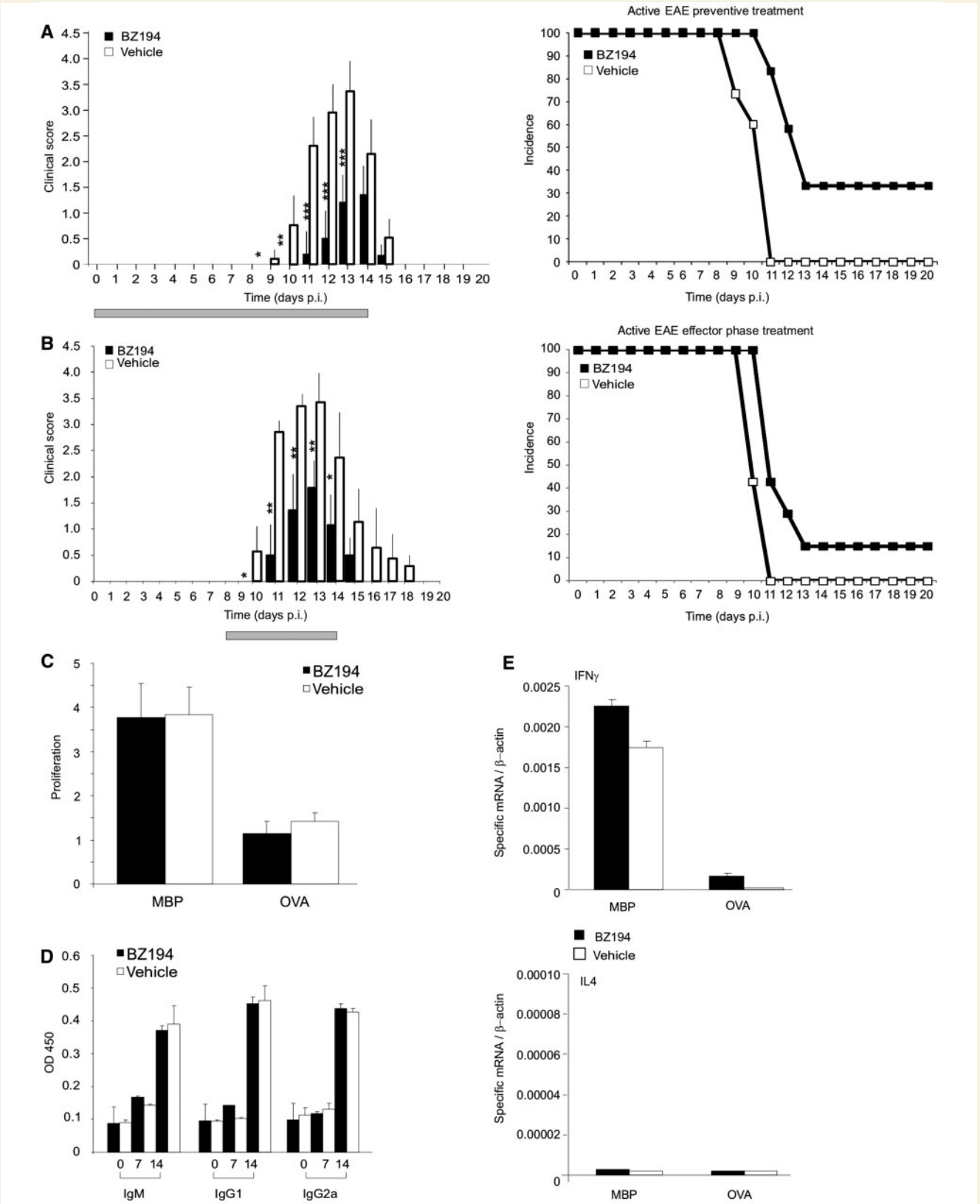

Figure 1 NAADP-antagonist BZ194 ameliorates active EAE without preventing primary immune responses. **(A** and **B)** Treatment of active EAE. Clinical course (left) and incidence rate (right; depicted as Kaplan–Meier curve) of active EAE after preventive (**A**; $n = 16$ animals/group) and effector phase (**B**; $n = 5$ animals/group) treatment with BZ194 (black) or vehicle (DMSO, white). Grey bar: period of treatment: Days 0–14 post injection (p.i.) (**A**), Days 8–14 p.i. (**B**). Cumulative data of three (**A**) and two (**B**) independent experiments are shown (means ± SD). *P*-values evaluated by Mann–Whitney rank statistical test: $*P \leq 0.05$, $**P \leq 0.001$, $***P \leq 0.0001$. **(C–E)** NAADP

Continued

Table 1 Treatment of active and adoptive transfer EAE with BZ194

Treatment	Number of analysed animals	Disease onset (days p.i.: active EAE; h p.t.: adoptive transfer EAE)	Disease duration (days: active EAE, hours: adoptive transfer EAE)	Max. mean clinical score	Clinical disease index	Max. body weight loss (%)[a]	Incidence (%)	Mortality (%)
Active EAE	Treatment Days 0–14							
BZ194	17	11 ± 0*	4.7 ± 0.6*	1.8 ± 0.1*	4.4 ± 3.7*	21 ± 11*	77	0
Nicotinic acid	5	10 ± 0	6 ± 0	3.9 ± 0.8	11.8 ± 3.6	47 ± 6	100	40
Vehicle	16	10 ± 0	6 ± 0	3.4 ± 0.4	11.9 ± 3	29 ± 0	100	33
Active EAE	Treatment Days 8–14							
BZ194	5	11*	5*	1.7*	4.8 ± 2.6*	20*	80	0
Vehicle	5	10	6	3.3	11.4 ± 0.5	32	100	0
Adoptive transfer EAE preventive	Treatment Days 0–4							
BZ194	22	84 ± 14*	138 ± 7*	1.6 ± 0.3*	5.1 ± 3.6*	12 ± 5*	82	0
Nicotinic acid	10	64 ± 22	168 ± 0	3.1 ± 0.1	12.6 ± 6.1	18 ± 1	100	0
Vehicle	22	67 ± 13	161 ± 11	3.2 ± 0.2	11.3 ± 7.2	17 ± 4	100	0
Untreated	8	67 ± 17	165 ± 5	3.0 ± 0.5	12.5 ± 6.1	20 ± 3	100	0
Adoptive transfer EAE therapeutic	Treatment Days 3–5							
BZ194	8	75 ± 2	43 ± 16*	1.9 ± 0.4	5 ± 1.5*	13 ± 3	100	0
Vehicle	8	72 ± 0	60 ± 16	2.1 ± 0.2	7.5 ± 1.6	13 ± 5	100	0

Preventive treatment of active EAE (Days 0–14 post injection): three independent experiments with BZ194 or vehicle treatment, one experiment with nicotinic acid. Treatment of active EAE during the effector phase (Days 8–14): one experiment with BZ194 and one experiment with vehicle. Adoptive transfer EAE (preventive treatment: Days 0–4): five independent experiments for BZ194 or vehicle treatment and three experiments with nicotinic acid application or untreated controls; two experiments with BZ194 or vehicle treatment for the therapeutic protocol (Days 3–5). Clinical disease index: cumulative clinical score over the entire disease course/rat.
a Maximal body weight loss: maximal body weight loss compared to the time of injection.
*P-value at least <0.05.

1999). BZ194 applied together with the T cells, or after onset of clinical signs, significantly suppressed clinical disease and CNS inflammation (Fig. 4A and B; Table 1; Supplementary Fig. 7).

Effector $T_{MBP\text{-}GFP}$ cells were reduced in their target organ in BZ194- compared to DMSO-treated control animals, while their numbers in spleen, lymph nodes and blood were increased (Fig. 4C; Supplementary Fig. 7A). These changes were most likely due to effects on the autoaggressive effector T cells: $T_{MBP\text{-}GFP}$ cells within the CNS showed strongly diminished expression of pro-inflammatory cytokines (Fig. 4D).

Notably, this reduced invasion of the attacked organs cannot be explained by the different expression of adhesion molecules and chemokine receptors of BZ194-treated effector T cells (Supplementary Fig. 8). Their capacity to follow chemotactic stimuli was not hindered by BZ194 treatment. C-X-C chemokine ligand (CXCL)10- and CCL5-induced migration of cultured and spleen-retrieved effector T cells was unchanged (Fig. 4E). Furthermore, BZ194 did not influence the invasion of brain-ignorant, OVA-reactive effector T cells into the inflammatory CNS lesions induced by intrathecal lipopolysaccharide-injection (Fig. 4F).

To confirm that reactivation of autoreactive effector T cells in their target organ is suppressed by BZ194 treatment, $T_{MBP\text{-}GFP}$ cells were loaded on spinal cord explants from early EAE lesions and their activation state tested 24 h later by measuring pro-inflammatory cytokine production. In the presence of BZ194, the $T_{MBP\text{-}GFP}$ cells produced significantly lower levels of IFNγ and interleukin-17 (Fig. 4G).

Interestingly, $T_{MBP\text{-}GFP}$ cells re-isolated from BZ194-treated animals fully retained their ability to respond to antigenic challenge

Figure 1 Continued
antagonism does not prevent primary immune responses. (**C**) Generation of T_{MBP} cells is not compromised by BZ194. Lymph node cells of BZ194-treated (black) or vehicle-treated (white) animals were isolated from draining lymph nodes 7 days p.i. with MBP, and their proliferative response to specific antigen tested by adding MBP (left bars) or OVA (right bars). Cell proliferation was evaluated 72 h later by (^{3}H)dT incorporation. Proliferation is indicated as the ratio between stimulated and non-stimulated cells. Data represent mean values ± SD of triplicate measurements. Representative data of five independent experiments including at least three animals per group. (**D**) MBP-specific antibody production remains unchanged after BZ194 treatment. Levels of anti-MBP antibodies within the serum of BZ194-treated (black) and vehicle-treated (white) animals were measured 0, 7 and 14 days p.i. with MBP. Data represent mean values ± SD of triplicate measurements. Representative data of two independent experiments including three animals per group. (**E**) BZ194 does not change the pro-inflammatory cytokine profile of T_{MBP} cells in draining lymph nodes Day 5 p.i. with MBP. Cytokine levels were determined by quantitative polymerase chain reaction in the cultured lymph node cells of BZ194-treated (black) and vehicle-treated (white) animals 48 h after addition of MBP or OVA. Representative data of three independent experiments. Ig = immunoglobulin; OD = optical density.

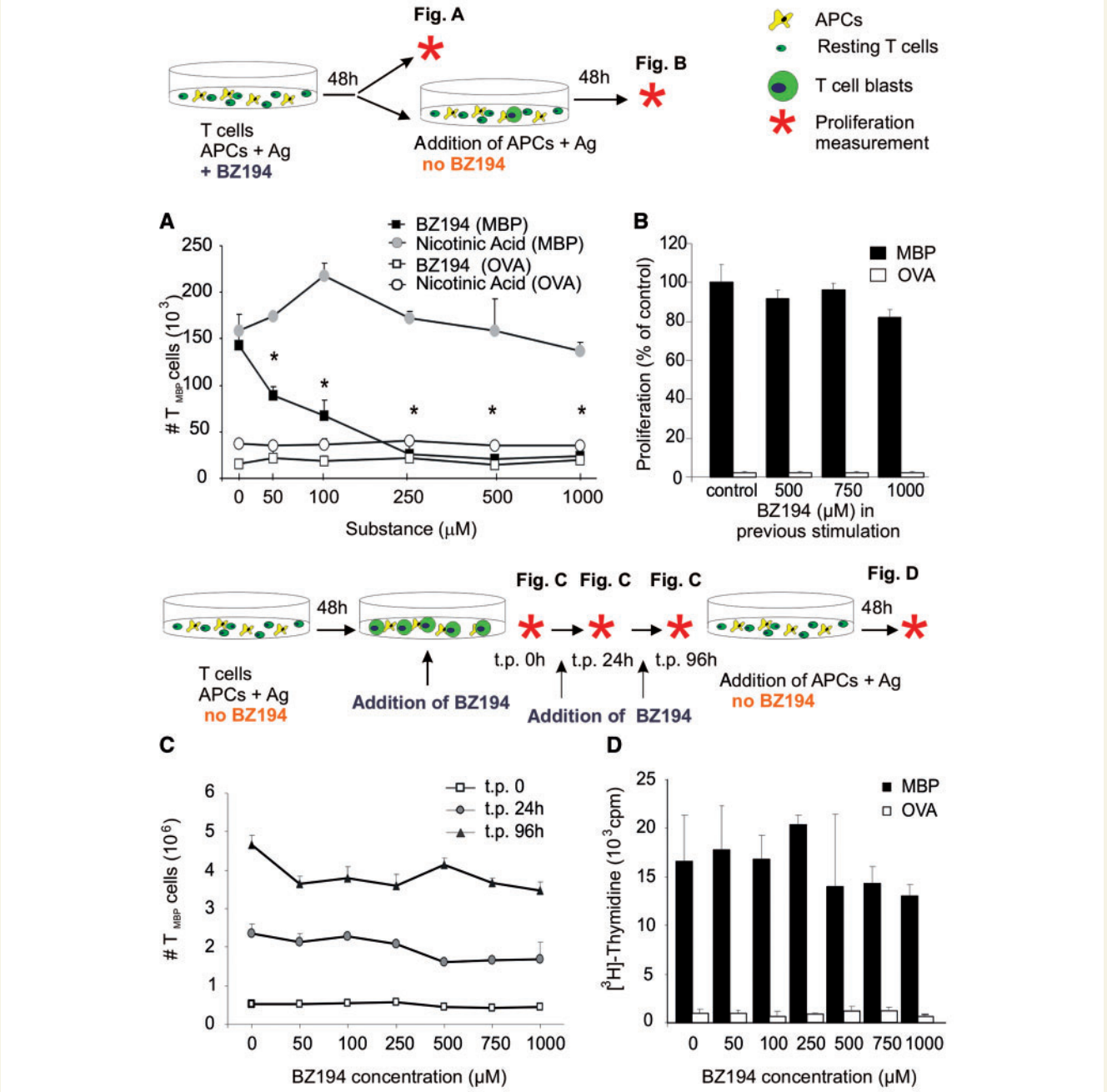

Figure 2 NAADP signalling is essential for efficient activation of (auto)antigen-specific T cells. (**A**) Anti-proliferative effect of BZ194 in $CD4^+$ effector T cells. Rat T_{MBP} cells co-cultured with MBP-pulsed antigen presenting cells (APCs; shaded) or control antigen (OVA) pulsed antigen presenting cells (unshaded) were incubated with increasing amounts of BZ194 (squares) or nicotinic acid (circles). Cell numbers were quantified by cytofluorometry 2 days later. Mean values ± SD of triplicate measurements. Representative data of 12 independent experiments. $*P \leq 0.0001$. (**B**) T_{MBP} cells previously stimulated in the presence of BZ194 for 2 days were re-exposed to MBP- or OVA-pulsed antigen presenting cells in the *absence* of BZ194. T_{MBP} cells reactivity was determined by (^{3}H)dT incorporation 2 days later. Proliferation is indicated as percent of control stimulated with MBP (resting T_{MBP} cells, MBP stimulation: 3256 ± 345 cpm; OVA stimulation: 76 ± 11 cpm). Mean values ± SD of triplicate measurements. Representative data of three independent experiments. (**C**) and (**D**) BZ194 is not toxic for T cells. (**C**) T_{MBP} cells were stimulated for 2 days with MBP-pulsed professional antigen presenting cells. Thereafter, the T cell blasts were incubated with the indicated amounts of BZ194. T_{MBP} cells were quantified 24 (grey circles) and 96 (black triangles) hours later by cytofluorometry. (**D**) After the 96 h-treatment with BZ194, the antagonist was washed out and the resting T_{MBP} cells were stimulated with specific (MBP, black) or control (OVA, white) antigen-pulsed antigen presenting cells. T_{MBP} cells reactivity was determined by (^{3}H)dT incorporation 3 days later. Values represent mean values ± SD of triplicate measurements. Representative data of three independent experiments. t.p. = time point.

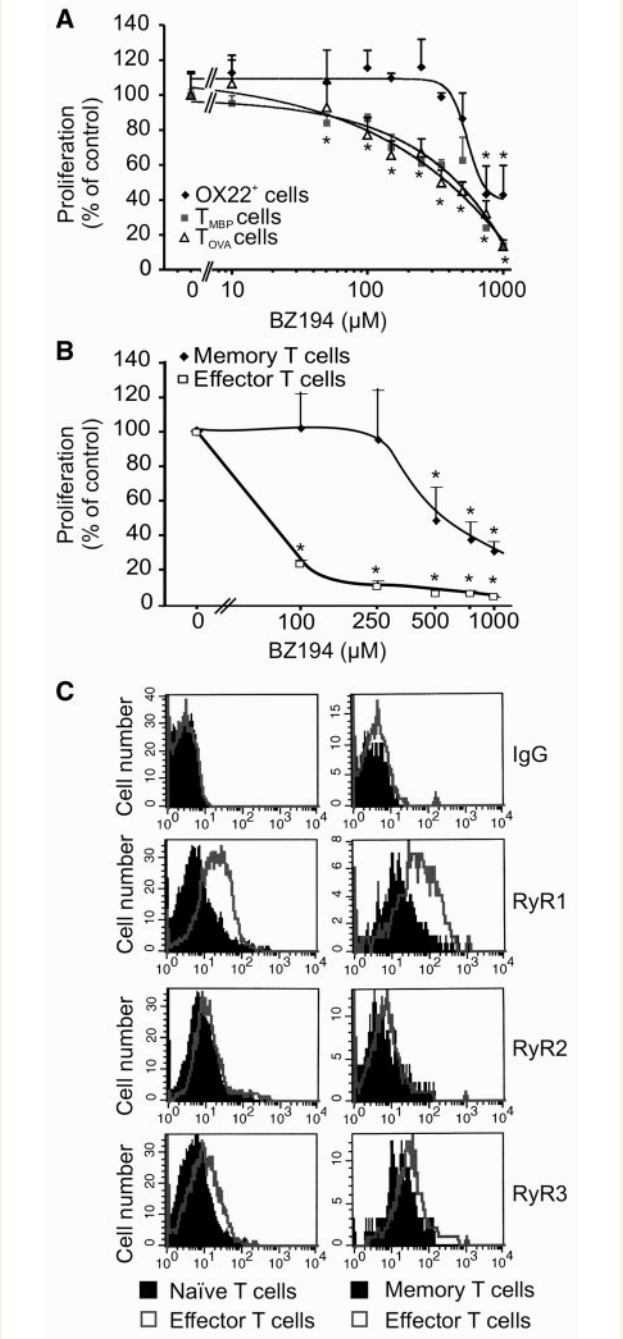

Figure 3 Effector T cells are more sensitive to NAADP antagonism than naïve and long lived memory T cells. (**A**) NAADP antagonism preferentially suppresses activation of antigen-experienced effector T cells. OX 22^{high} (OX 22^{+}) naïve T cells (black) or effector T cells (T_{MBP} cells, grey and T_{OVA} cells, white) were activated with anti-CD3/CD28 antibody in the presence of the indicated amounts of BZ194. (**A**) The proliferative response was determined 2 days later by (^{3}H)dT incorporation. For better comparability, proliferation is indicated as a percentage of non-treated naïve (4658 ± 249 cpm) and effector T cells (T_{MBP} 7391 ± 232 cpm, T_{OVA} 6490 ± 272 cpm), respectively. Data represent mean values ± SD of triplicate measurements. Representative data of three independent experiments. *$P \leq 0.01$. (**B**) Memory T cells are less susceptible to NAADP antagonism than effector T cells. Shown are the effects of increasing amounts of BZ194 on antigen-specific proliferation of $T_{OVA\text{-}GFP}$ memory (black) or $T_{OVA\text{-}GFP}$ effector (white) cells. Quantification of cell numbers was performed by cytofluorometry 2 days later. Proliferation is indicated as percent of control (no BZ194 treatment). Data represent means ± SD of three measurements from two independent experiments. *$P \leq 0.05$. (**C**) Cytofluorometrical quantification of ryanodine receptor 1–3 in naïve T cells (shaded histograms, left panel) and memory T cells (shaded histograms, right panel) compared to effector T_{MBP} cells (open overlay histograms). Representative data of at least three independent experiments. RyR = ryanodine receptor; Ig = immunoglobulin.

when cultured in the absence of the antagonist (Supplementary Fig. 9). These data confirm the previous observation that BZ194 interferes with re-activation of the effector T cells by rendering the cells reversibly non-responsive (Fig. 2B; Supplementary Fig. 4E).

Intravital imaging of BZ194-treated effector $T_{MBP\text{-}GFP}$ cells

Using intravital two-photon laser scanning microscopy, we studied the effector T cell behaviour *in situ* (Kawakami *et al*., 2005*a*; Odoardi *et al*., 2007*a*; Bartholomäus *et al*., 2009). We recently detected that $T_{MBP\text{-}GFP}$ cells in the EAE lesions displayed characteristic locomotion patterns: 35% of the infiltrated $T_{MBP\text{-}GFP}$ cells were stationary in the target tissue, i.e. they were fixed to anchor points reminiscent of cells in the process of antigen recognition; the other portion of cells (65%) was motile and moved with high velocity through the compact CNS tissue (Fig. 5A–D) (Kawakami *et al*., 2005*a*). In BZ194-treated animals, we observed similar locomotion patterns; however, a higher fraction (>80%) of the effector T cells were motile in the meninges and the adjacent dorsal spinal cord parenchyma, whereas only <20% were stationary (Fig. 5A–D; Supplementary Videos 1 and 2). Furthermore, the average velocity of the effector T cells within the EAE lesions was increased (Fig. 5E). An analysis of individual cell trajectories, instantaneous velocities and meandering indices (a measure of the straightness of T cell movement) revealed that this increased velocity after BZ194 treatment was not due to altered locomotion characteristics of motile effector T cells, but rather because the number of arresting T cells was decreased compared to controls (Fig. 5). These data were confirmed in acute spinal cord explants, which allowed imaging throughout the cross-section of the spinal cord (Fig. 5; Supplementary Videos 3 and 4).

Discussion

Autoimmune diseases are evoked by T cells reactive against specific autoantigens, which are presented in the attacked organs. The acute phase of any autoimmune disease is initiated when autoaggressive effector T cells invade their target organs and become locally reactivated upon encountering the specific antigen. The ensuing release of pro-inflammatory mediators sets the stage for recruitment of further immune cells and the onset of clinical

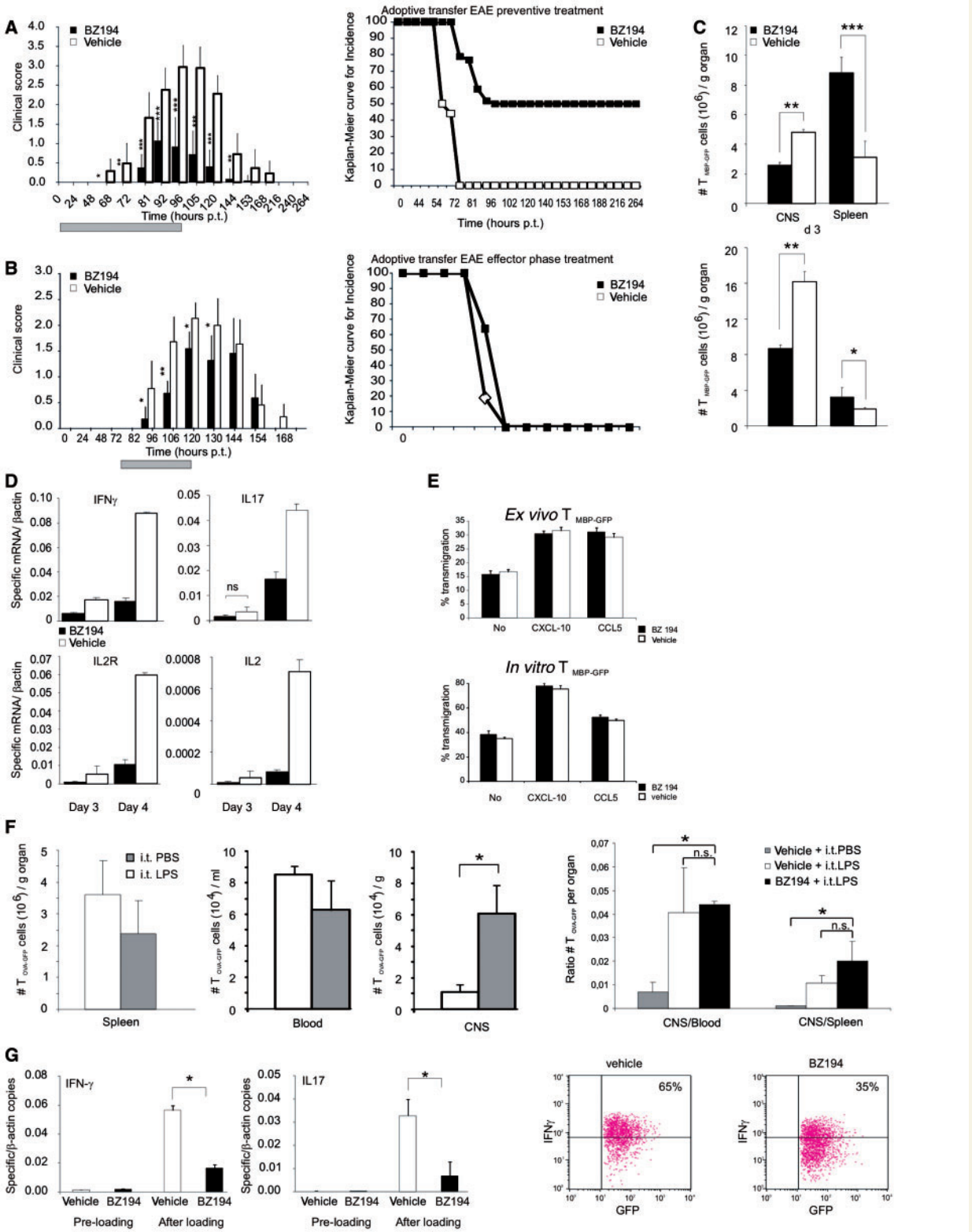

Figure 4 NAADP-antagonist interferes with $T_{MBP\text{-}GFP}$ cell activation within the CNS. (**A** and **B**) Treatment of adoptive transfer EAE. Clinical course (left) and disease incidence (right; Kaplan–Meier curve) of EAE after transfer of $T_{MBP\text{-}GFP}$ cells**.** Treatment performed with preventive schedule (**A;** $n = 22$ animals/group) and during effector phase (**B**; $n = 8$ animals/group) with BZ194 (black) or vehicle (DMSO, white). Grey bar: period of treatment: 0–96 h post transfer (p.t.) (**A**); 72–120 h p.t. (**B**). Cumulative data of five (**A**) and three (**B**) independent experiments are shown (mean values ± SD). *P*-values measured by Mann–Whitney rank statistical test: $*P \leq 0.01$, $**P \leq 0.001$, $***P \leq 0.0001$. (**C**) BZ194 reduces homing of encephalitogenic effector T cells into their target organ. Cytofluorometric quantification of $T_{MBP\text{-}GFP}$ cells in the spinal cord (CNS) or the spleen of BZ194-treated (black) or vehicle-treated (white) animals 3 days (upper panel) and 4 days (lower panel) p.t. Values represent mean values ± SD of triplicate measurements. Representative data of five

Continued

disease (Kawakami *et al.,* 2004; Becher *et al.,* 2006; Odoardi *et al.,* 2007*a*; Bartholomäus *et al.,* 2009).

Here, we tested a novel strategy to interfere with the activation of autoaggressive effector T cells. To this end, we used BZ194, a recently developed antagonist, which specifically interferes with NAADP-mediated Ca^{2+} signalling in T cells (Langhorst *et al.,* 2004; Dammermann, *et al.,* 2009). The NAADP antagonist was applied in EAE of the Lewis rat, a model for multiple sclerosis. First preliminary results indicate that BZ194 is similarly effective in experimental autoimmune neuritis of the Lewis rat, a model for Guillain-Barré syndrome (Hartung *et al.,* 1988) that is induced by transfer of P2-reactive effector T cells (data not shown). The EAE and experimental autoimmune neuritis models are particularly well suited to test T cell-directed therapies, since their pathologies are strictly dependent on autoaggressive T cells. Furthermore, their unrivalled reproducibility together with the possibility to use genetically labelled autoaggressive effector T cells allowed us to track as well as to characterize functionally the disease-inducing cell populations throughout the disease course (Flügel *et al.,* 1999; Kawakami *et al.,* 2004, 2005*a*; Odoardi *et al.,* 2007*b*).

BZ194 treatment significantly ameliorated clinical symptoms and autoimmune inflammation in EAE. Autoreactive effector T cells within CNS lesions showed reduced activatory levels upon treatment with BZ194 and their numbers within the target organ were reduced. Instead, the T cells accumulated within secondary lymph organs and the blood (Fig. 4C; Supplementary Fig. 7A). Autoaggressive $T_{MBP\text{-}GFP}$ cells during preclinical EAE were found to migrate first to lymph nodes and then to the spleen, before they reached, via the blood, their target organ, where they were stimulated to produce pro-inflammatory cytokines (Flügel *et al.,* 2001; Kawakami *et al.,* 2004; Odoardi *et al.,* 2007*b*). Brain antigen-ignorant T cells (T_{OVA} cells), in contrast, did not spontaneously invade the brain tissue, but rather re-circulated within the blood and secondary lymphatic tissues (Flügel *et al.,* 2001). Thus, the migratory behaviour of the T_{MBP} cells after BZ194 treatment resembled the behaviour of brain antigen-ignorant T cells. These observations and the findings that BZ194-treated effector T cells readily respond to chemokine stimuli argue for the case that BZ194 does not directly interfere with the migratory capacity of effector T cells in peripheral lymphoid organs.

During EAE, the autoaggressive effector T cells enter their target organ from leptomeningeal vessels where they come into contact with menigeal/perivascular macrophages capable of presenting myelin antigens (Bartholomäus *et al.,* 2009; Kivisäkk *et al.,* 2009). These encounters and the ensuing reactivation of the effector T cells were found to be essential for their penetration into the CNS parenchyma (Bartholomäus *et al.,* 2009). Notably, $T_{MBP\text{-}GFP}$ cells, which arrived at their target organ during BZ194 treatment, did not distribute evenly throughout the CNS parenchyma but were rather preferentially located in leptomeningeal and perivascular areas (Supplementary Fig. 7C). A similar cell distribution was found in EAE lesions of animals in which local antigen presentation was prevented by elimination of resident antigen presenting cells via application of clodronate containing liposomes (Tran *et al.,* 1998).

Contacts between autoreactive effector T cells and resident antigen presenting cells in the CNS were changed after BZ194 treatment (Fig. 5). The percentage of T cells continuously strolling through the CNS tissue was substantially increased, whereas the amount of T cells with restricted motility that has been shown to be in contact with antigen presenting cells (Kawakami *et al.,* 2005*a*; Bartholomäus *et al.,* 2009) was decreased. Recent live imaging studies indicate that T cell contacts to antigen presenting cells are regulated by Ca^{2+} fluxes resulting from antigen encounters. Thus, the arrest of thymocytes during positive selection and deceleration of naïve T cells in contact with antigen loaded dendritic cells was found to be dependent on intracellular Ca^{2+} elevation (Bhakta *et al.,* 2005; Skokos *et al.,* 2007).

Figure 4 Continued
independent experiments. *P*-values: $*P \leq 0.05$, $**P \leq 0.01$, $***P \leq 0.005$. (**D**) NAADP signalling is essential for efficient re-activation of effector $T_{MBP\text{-}GFP}$ cells within their target organ. Reduced expression of pro-inflammatory mediators in autoaggressive $T_{MBP\text{-}GFP}$ cells within the CNS after BZ194 treatment. Quantitative PCR of $T_{MBP\text{-}GFP}$ cells sorted from spinal cords 3 and 4 days p.t. Black bars: BZ194-treated; white bars: vehicle-treated animals. Values are normalized to β-actin mRNA. Representative data of three independent experiments. All differences are statistically significant (*P*-value at least ≤ 0.05) unless otherwise specified. ns, not significant. (**E** and **F**) BZ194 treatment does not interfere with migration capacity of *ex vivo*, *in vitro* or *in vivo* effector T cells. (**E**) $T_{MBP\text{-}GFP}$ cells were isolated *ex vivo* from spleens (upper plots) of animals treated with BZ194 (0.5 mM) (black bars) or vehicle (white bars) at Day 3 p.t., or cultured (lower plots) for 3 days in presence of the inhibitor (black bars) or vehicle (white bars). Percentage of transmigration without or in presence of the indicated chemokines was assessed by cytofluorometry 6 h after plating. (**F**) Three days after transfer of 2.5×10^6 effector $T_{OVA\text{-}GFP}$ cells, animals were intrathecally (i.t.) injected with 150 ng of lipopolysaccharide (LPS) (white bars) or equal volume of phosphate buffered saline (PBS) (grey bars); 24 h later, the numbers of GFP positive cells were determined in the spleen (left plot), blood and spinal cord (CNS; middle plot) by flow cytometry. Right plot: adoptive transfer of effector $T_{OVA\text{-}GFP}$ cells was performed as above. The animals received a daily i.p. injection of BZ194 or vehicle from Days 0 to 3 p.t. At the Day 3 p.t. BZ194-treated (black bars) and vehicle-treated (white bars) animals were i.t. injected with lipopolysaccharide; for control, vehicle-treated animals were also i.t. injected with phosphate buffered saline (grey bars). The graph shows ratios of total number of GFP-positive cells detected in the spinal cord (CNS) relative to the numbers in the blood (left) or in the spleen (right) on Day 4 p.t. $*P < 0.05$; n.s. = not significant. (**G**) BZ194 treatment reduces the activation of effector T cells on CNS explants. $T_{MBP\text{-}GFP}$ cells were cultured for 2 h in presence of BZ194 (black bars, pre-loading) or vehicle (white bars, pre-loading) and then loaded on spinal cord explants from mild EAE animals (after loading) in presence of the antagonist (0.5 mM; black bars) or of the vehicle (white bars). Twenty-four hours later, $T_{MBP\text{-}GFP}$ cells were sorted out and the levels of IFNγ (left graph) and interleukin-17 (right graph) were measured by quantitative polymerase chain reaction. Representative data of three independent experiments are shown. Values normalized to β-actin mRNA. $*P < 0.05$. Right dot plots: corresponding protein expression of IFN-γ, evaluated by flow cytometry of $T_{MBP\text{-}GFP}$ cells isolated from spinal cord explants 36 h after loading.

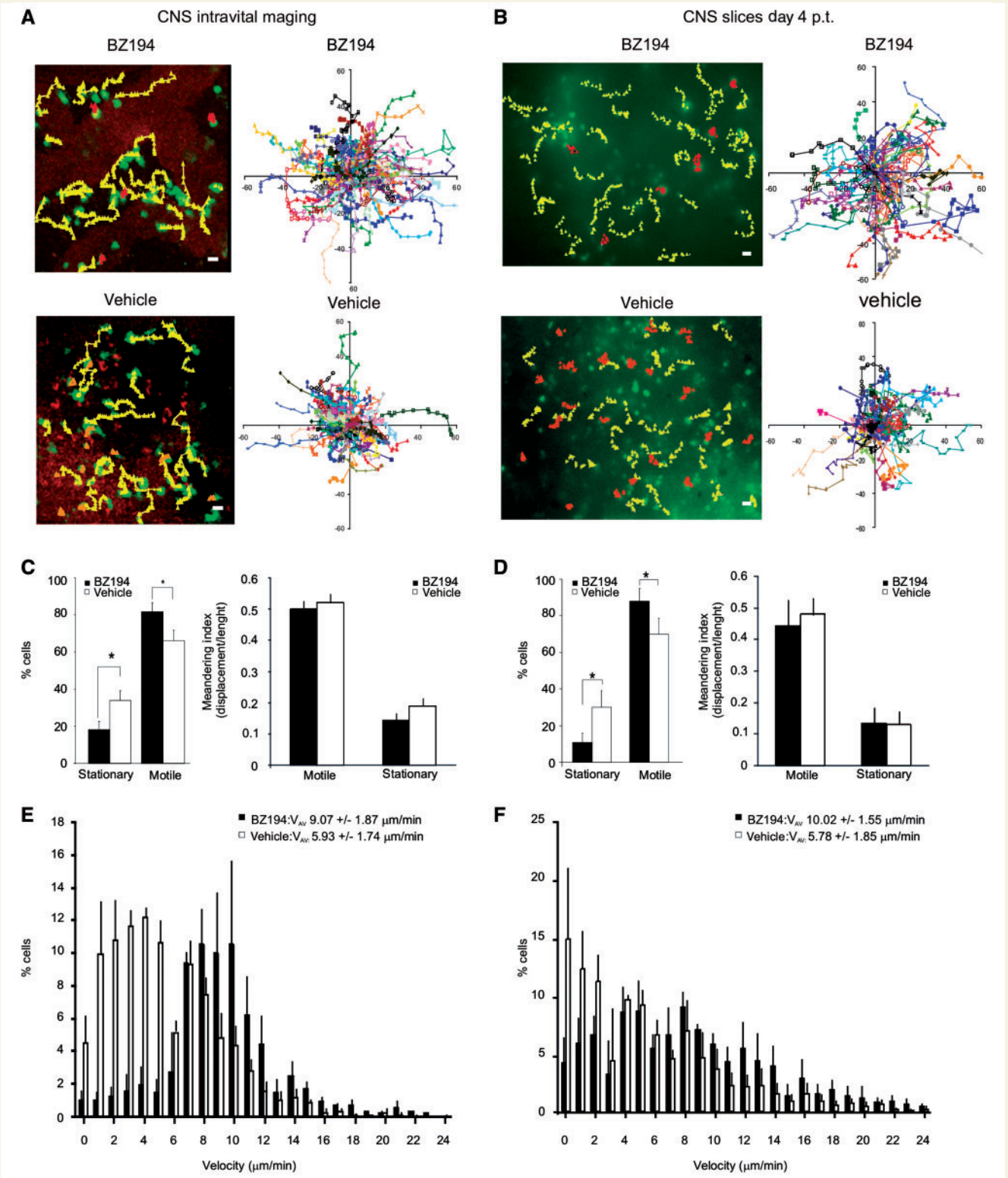

Figure 5 BZ194 increases effector T cell motility within EAE lesions. The locomotion patterns of $T_{MBP\text{-}GFP}$ cells in EAE lesions at Day 4 p.t. were analysed in real time within the spinal cord using intravital two-photon laser scanning microscopy (**A**, **C** and **E**), or within spinal cord explants using two-photon laser scanning microscopy or video fluorescence microscopy (**B**, **D** and **F**). (**A** and **B**, left panels) The trajectories of representative stationary (orange) and motile (yellow) $T_{MBP\text{-}GFP}$ cells in BZ194-treated (upper panels) or vehicle-treated (lower panels) animals are shown: (**A**) intravital imaging; (**B**) spinal cord explant analyses (**B**); motile cells: displacements >10 µm/10 min; stationary cells: displacements <10 µm/10 min. Magnification bar = 10 µm. (**A** and **B**, right panels) Superimposed trajectories are shown. Each coloured line represents one cell. (**A**) Intravital analyses: two representative two-photon laser scanning microscopy movies comprising 88 (BZ194-treatment) and 85 (vehicle-treatment) $T_{MBP\text{-}GFP}$ cells are shown. (**B**) Spinal cord explants: two representative video microscopy

Continued

At present, we cannot completely rule out that NAADP antagonism acts on additional cell populations or T cell functions, e.g. their interaction with other cells or with the extracellular matrix. First experiments involving neuronal cells (Supplementary Fig. 10) and glial cell cultures (Cordiglieri *et al*., results not published) did not reveal any clear effects of BZ194 treatment on functional or structural properties of neural cells. The function of antigen presenting cells seems evenly unchanged upon BZ194 treatment (Supplementary Figs 2 and 5). Therefore, our data strongly suggest that the clinical effects of BZ194 are due to inefficient re-activation of the autoaggressive effector T cells within their target organ.

Previous studies indicated a complex T cell receptor-triggered Ca^{2+} signalling network regulated by tightly controlled metabolisms and synergisms of NAADP (Gasser *et al*., 2006), IP_3 (Guse *et al.,* 1995) and cyclic ADP-ribose (Guse *et al.,* 1999). Thereby it was suggested that NAADP, which peaks within seconds after T cell receptor activation, acts as the initializing trigger supporting later Ca^{2+} release events by amplifying IP_3- and cyclic ADP-ribose-induced Ca^{2+} release (Gasser *et al*., 2006). IP_3 appeared within a few minutes (Guse *et al*., 1995) followed by cyclic ADP-ribose within tens of minutes, respectively (Guse *et al.,* 1999). Why do T cells need such a complex signalling network to fine tune Ca^{2+} responses? The decision of whether to continue or to stop Ca^{2+} signalling may ultimately result in cell proliferation and exertion of effector functions, or it may drive the T cell into a state of unresponsiveness or cell death. The NAADP/Ca^{2+} signalling pathway seems to control this decision, since expression of the major cytokine involved in T cell proliferation, interleukin-2, depends on a full, NAADP-initiated Ca^{2+} response. If the NAADP pathway is blocked, Ca^{2+} signalling is only partially activated. Therefore, it does not provide a sufficiently long-lasting increase in the free cytosolic Ca^{2+} to allow Ca^{2+}/calmodulin- and calcineurin-dependent translocation of nuclear factor of activated T cells (NFAT) into the nucleus (Timmerman *et al.,* 1996; Dammermann *et al.,* 2009). Expression of the pro-inflammatory cytokines IFN-γ and interleukin-17 was evenly suppressed by BZ194 indicating that Ca^{2+} signalling initiated by NAADP is also involved in these signalling cascades.

Notably, BZ194 did not exert toxic effects. Effector T cells re-isolated from BZ194-treated animals readily reacted towards exposure to specific antigen after wash-out of the antagonist. Obviously, this wash-out of BZ194, when analysed in cultured or *ex vivo*-isolated effector T cells was very rapid, which explains the immediate reactivity of the effector T cells after withdrawal of the antagonist (Supplementary Fig. 11). Thus, blocking NAADP-mediated Ca^{2+} signalling by BZ194 at the very early state of T cell activation seems to induce a state of transient non-responsiveness in the effector T cells. The observed strong elevations of the transcription factors egr-2 and -3, which have been recently identified as potent regulators of T cell anergy (Safford *et al.,* 2005), point in this direction.

Ryanodine receptor 1 was recently identified as the putative receptor for NAADP in effector T cells (Dammermann *et al.,* 2009). Our data indicate that T cells regulate this receptor according to their functional state, which could explain the different susceptibility to BZ194 inhibition. We found higher expression levels in effector T cells compared to naïve and long-lived memory T cells (Fig. 3C). Correlating with their low ryanodine receptor 1 levels, naïve T cells *in vitro* were suppressed only at BZ194-concentrations of $>750\,\mu M$ (Fig. 3A; Supplementary Fig. 6B). Similar observations were made with long-lived memory T cells (Fig. 3B; Supplementary Fig. 6B). At the concentrations observed *in vivo* ($\sim 300\,\mu M$, Supplementary Fig. 12) primary immune responses, i.e. the generation of specific effector T and B cells, were unhindered (Fig. 1C–E). This is of therapeutic relevance, since the antagonist seemed to interfere selectively with the function of antigen-primed effector T cells that are inhibited at more than 10-fold lower levels of BZ194.

Current T cell-directed therapies in autoimmune disorders based on synthetic peptides or altered peptide ligands aim to modulate T cellular functions and to convert a pro-inflammatory T_H1 response into an anti-inflammatory T_H2 or T_H3 driven immunity (Aharoni *et al.,* 1997; Weiner, 2004; Fontoura *et al.,* 2005). Alternative strategies interfere with antigen presentation to T cells or T cell migration into their target organ (Miller *et al.,* 2003; Kappos *et al.,* 2006; Markowitz, 2007). However, all endeavours have been either insufficient in dampening down the

Figure 5 Continued
recordings including 52 (BZ194) and 50 (vehicle) $T_{MBP\text{-}GFP}$ cells are shown. (**C** and **D**) Characterization of motile and stationary cells. (**C** and **D**, left panels) Quantifications of motile and stationary $T_{MBP\text{-}GFP}$ cells in BZ194-treated (black) versus vehicle-treated (white) animals. Data from intravital analyses represent mean values ± SD of three independent movies including 255 cells and 16 065 time intervals per treatment (**C**); explant video microscopy data represent mean values ± SD of five independent movies including 304 cells and 31 920 time intervals per treatment (**D**). $^*P \leq 0.05$. (**C** and **D**, right panels) The graphs show the meandering indices of $T_{MBP\text{-}GFP}$ cells of BZ194-treated or vehicle-treated animals. The meandering index is calculated as total cell displacement divided by the path length of a cell track. Intravital analyses: 340 cells in BZ194- and 223 cells in vehicle-treated animals were analysed. Values represent means ± SD from three independent movies/treatment**.** Spinal cord explant analyses: 154 cells in BZ194-treated and 228 cells in vehicle-treated animals were analysed. Mean values ± SD from five independent movies/treatments, including three video-microscopy movies and two two-photon laser scanning microscopy recordings are shown. (**E** and **F**) Instantaneous velocities of $T_{MBP\text{-}GFP}$ cells in the EAE lesions. (**E**) Intravital imaging: velocities of $T_{MBP\text{-}GFP}$ cells in BZ194-treated (black bars; total 340 cells; 8160 time points) or vehicle-treated (white bars; total 223 cells; 5352 time points) animals are shown. Data represent means ± SD from three independent movies/treatment. (**F**) Instantaneous velocities of $T_{MBP\text{-}GFP}$ cells in spinal cord explants of BZ194-treated (black bars; total 154 cells; 3696 time points) or vehicle-treated (white bars; total 228 cells; 5472 time points) animals. Mean values ± SD from five independent movies/treatment including three video microscopy movies and two two-photon laser scanning microscopy recordings are depicted. Average velocities (V_{AV}) are indicated.

inflammation or have completely blocked immune processes, promoting the risk of infectious complications, i.e. progressive multifocal leucoencephalopathy after application of anti-Very Late antigen-4 (a_4b_1 integrin) (VLA4) antibody (Langer-Gould and Steinman, 2006). Interfering with Ca^{2+} signalling as an early and essential component of T cell activation might represent an alternative and promising therapeutic approach, as is also indicated by recent studies using specific inhibitors of the potassium channels Kv1.3 or TWIK-related acid-sensitive potassium channel 1 (TASK1) (Beeton *et al.,* 2001, 2006; Bittner *et al.,* 2009). These inhibitors indirectly affect Ca^{2+} signalling by modulating the long-lasting plateau phase (Beeton *et al.,* 2001). NAADP as a direct participant in the Ca^{2+} signalling machinery might serve as a novel potential therapeutic target. NAADP antagonists interfered preferentially with the function of antigen-experienced effector T cells. Of note is that this also included human autoantigen-specific T cells. Furthermore, BZ194 ameliorated autoimmune diseases not only when given before the onset of the symptoms, but also afterwards, even though the observed therapeutic effects were less pronounced, most likely due to the fact that the CNS invasion of the myelin-reactive effector T cells and their local reactivation already starts during the preclinical phase of EAE (Bartholomäus *et al.,* 2009). These observed features of BZ194 may ultimately be beneficial for the treatment of human patients with autoimmune diseases, and point to the necessity of exploring this novel therapeutic approach in future.

Acknowledgements

The authors thank Ingeborg Haarmann, Christine Federle, Simone Hamann and Adriane Stas for technical assistance. We thank Cathy Ludwig for excellent secretarial help. We are grateful to Dr Cinthia Farina for her input in the establishment of neural cell cultures. We thank Dr Henrike Körner for her support with in intrathecal injections.

Funding

This work was supported by the Gemeinnützige Hertie foundation (grant no. 1.01.1/04/010 and 1.01.1/07/005 to A.F. and A.H.G.), the Deutsche Forschungsgemeinschaft (SFB-TR-43 and FOR1336 to A.F., SFB571 to K.D., GU360/7-1,7-2,7-3,7-5 and GU360/13-1 to A.H.G.), the Bundesministerium für Bildung und Forschung ('Understanding Multiple Sclerosis heterogeneity: linking human disease with animal models—UNDERSTAND MS' to A.F.), an Enterprise Development Grant from the University of Bath (to B.V.L.P.), and the Wellcome Trust (Biomedical Research Collaboration grant no. 068065 to B.V.L.P. and A.H.G.).

Supplementary material

Supplementary material is available at *Brain* online.

References

Aharoni R, Teitelbaum D, Sela M, Arnon R. Copolymer 1 induces T cells of the T helper type 2 that cross-react with myelin basic protein and suppress experimental autoimmune encephalomyelitis. Proc Natl Acad Sci USA 1997; 94: 10821–6.

Bartholomäus I, Kawakami N, Odoardi F, Schläger C, Miljkovic D, Ellwart JW, et al. Effector T cell interactions with meningeal vascular structures in nascent autoimmune CNS lesions. Nature 2009; 462: 94–8.

Becher B, Bechmann I, Greter M. Antigen presentation in autoimmunity and CNS inflammation: how T lymphocytes recognize the brain. J Mol Med 2006; 84: 532–43.

Beeton C, Wulff H, Barbaria J, Clot-Faybesse O, Pennington M, Bernard D, et al. Selective blockade of T lymphocyte K^+ channels ameliorates experimental autoimmune encephalomyelitis, a model for multiple sclerosis. Proc Natl Acad Sci USA 2001; 98: 13942–7.

Beeton C, Wulff H, Standifer NE, Azam P, Mullen KM, Pennington MW, et al. Kv1.3 channels are a therapeutic target for T cell-mediated autoimmune diseases. Proc Natl Acad Sci USA 2006; 103: 17414–9.

Ben-Nun A, Wekerle H, Cohen IR. The rapid isolation of clonable antigen-specific T lymphocyte lines capable of mediating autoimmune encephalomyelitis. Eur J Immunol 1981; 11: 195–9.

Berg I, Potter BVL, Mayr GW, Guse AH. Nicotinic acid adenine dinucleotide phosphate (NAADP(+)) is an essential regulator of T-lymphocyte Ca(2+)-signaling. J Cell Biol 2000; 150: 581–8.

Bhakta NR, Oh DY, Lewis RS. Calcium oscillations regulate thymocyte motility during positive selection in the three-dimensional thymic environment. Nat Immunol 2005; 6: 143–51.

Bittner S, Meuth SG, Göbel K, Melzer N, Herrmann AM, Simon OJ, et al. TASK1 modulates inflammation and neurodegeneration in autoimmune inflammation of the central nervous system. Brain 2009; 132: 2501–16.

Dammermann W, Zhang B, Nebel M, Cordiglieri C, Odoardi F, Kirchberger T, et al. NAADP-mediated Ca^{2+} signaling via type 1 ryanodine receptor in T cells revealed by a synthetic NAADP antagonist. Proc Natl Acad Sci USA 2009; 106: 10678–83.

Feske S, Gwack Y, Prakriya M, Srikanth S, Puppel SH, Tanasa B, et al. A mutation in Orai1 causes immune deficiency by abrogating CRAC channel function. Nature 2006; 441: 179–85.

Flügel A, Berkowicz T, Ritter T, Labeur M, Jenne D, Li Z, et al. Migratory activity and functional changes of green fluorescent effector T cells before and during experimental autoimmune encephalomyelitis. Immunity 2001; 14: 547–60.

Flügel A, Willem M, Berkowicz T, Wekerle H. Gene transfer into $CD4^+$ T lymphocytes: green fluorescent protein engineered, encephalitogenic T cells used to illuminate immune responses in the brain. Nature Med 1999; 5: 843–7.

Fontoura P, Garren H, Steinman L. Antigen-specific therapies in multiple sclerosis: going beyond proteins and peptides. Int Rev Immunol 2005; 24: 415–46.

Gasser A, Bruhn S, Guse AH. Second messenger function of nicotinic acid adenine dinucleotide phosphate revealed by an improved enzymatic cycling assay. J Biol Chem 2006; 281: 16906–13.

Guse AH, da Silva CP, Berg I, Skapenko AL, Weber K, Heyer P, et al. Regulation of calcium signalling in T lymphocytes by the second messenger cyclic ADP-ribose. Nature 1999; 398: 70–3.

Guse AH, Goldwich A, Weber K, Mayr GW. Non-radioactive, isomer-specific inositol phosphate mass determinations: high-performance liquid chromatography-micro-metal-dye detection strongly improves speed and sensitivity of analyses from cells and micro-enzyme assays. J Chromatogr B Biomed Appl 1995; 672: 189–98.

Hartung H-P, Heininger K, Schäfer B, Fierz W, Toyka KV. Immune mechanisms in inflammatory neuropathy. Ann NY Acad Sci 1988; 540: 122–61.

Kappos L, Antel J, Comi G, Montalban X, O'Connor P, Polman CH, et al. Oral fingolimod (FTY720) for relapsing multiple sclerosis. N Engl J Med 2006; 355: 1124–40.

Kawakami N, Lassmann S, Li Z, Odoardi F, Ritter T, Ziemssen T, et al. The activation status of neuroantigen-specific T cells in the target organ determines the clinical outcome of autoimmune encephalomyelitis. J Exp Med 2004; 199: 185–97.

Kawakami N, Nägerl UV, Odoardi F, Bonhoeffer T, Wekerle H, Flügel A. Live imaging of effector cell trafficking and autoantigen recognition within the unfolding autoimmune encephalomyelitis lesion. J Exp Med 2005a; 201: 1805–14.

Kawakami N, Odoardi F, Ziemssen T, Bradl M, Ritter T, Neuhaus O, et al. Autoimmune $CD4^+$ T cell memory: Lifelong persistence of encephalitogenic T cell clones in healthy immune repertoires. J Immunol 2005b; 175: 69–81.

Kivisäkk P, Imitola J, Rasmussen S, Elyaman W, Zhu B, Ransohoff RM, et al. Localizing central nervous system immune surveillance: meningeal antigen-presenting cells activate T cells during experimental autoimmune encephalomyelitis. Ann Neurol 2009; 65: 457–69.

Langer-Gould A, Steinman L. Progressive multifocal leukoencephalopathy and multiple sclerosis: lessons from natalizumab. Curr Neurol Neurosci Rep 2006; 6: 253–8.

Langhorst MF, Schwarzmann N, Guse AH. Ca^{2+} release via ryanodine receptors and Ca^{2+} entry: major mechanisms in NAADP-mediated Ca^{2+} signaling in T-lymphocytes. Cell Signal 2004; 16: 1283–9.

Markowitz CE. Interferon-beta: mechanism of action and dosing issues. Neurol 2007; 68: S8–11.

Miller DH, Khan OA, Sheremata WA, Blumhardt LD, Rice GP, Libonati MA, et al. A controlled trial of Natalizumab for relapsing multiple sclerosis. N Engl J Med 2003; 348: 15–23.

Odoardi F, Kawakami N, Klinkert WE, Wekerle H, Flügel A. Blood-borne soluble protein antigen intensifies T cell activation in autoimmune CNS lesions and exacerbates clinical disease. Proc Natl Acad Sci USA 2007a; 104: 18625–30.

Odoardi F, Kawakami N, Li Z, Cordiglieri C, Streyl K, Nosov M, et al. Instant effect of soluble antigen on effector T cells in peripheral immune organs during immunotherapy of autoimmune encephalomyelitis. Proc Natl Acad Sci USA 2007b; 104: 920–5.

Peinelt C, Vig M, Koomoa DL, Beck A, Nadler MJ, Koblan-Huberson M, et al. Amplification of CRAC current by STIM1 and CRACM1 (Orai1). Nat Cell Biol 2006; 8: 771–3.

Powrie F, Mason D. Phenotypic and functional heterogeneity of CD4+ T cells. Immunol Today 1988; 9: 274–7.

Ramírez F, Mason D. Recirculatory and sessile $CD4^+$ T lymphocytes differ on CD45RC expression. J Immunol 2000; 165: 1816–23.

Safford M, Collins S, Lutz MA, Allen A, Huang CT, Kowalski J, et al. Egr-2 and Egr-3 are negative regulators of T cell activation. Nat Immunol 2005; 6: 472–80.

Skokos D, Shakhar G, Varma R, Waite JC, Cameron TO, Lindquist RL, et al. Peptide-MHC potency governs dynamic interactions between T cells and dendritic cells in lymph nodes. Nat Immunol 2007; 8: 835–44.

Steinman L, Waisman A, Altmann D. Major T cell responses in multiple sclerosis. Mol Med Today 1995; 1: 79–83.

Streb H, Irvine RF, Berridge MJ, Schulz I. Release of Ca^{2+} from a non-mitochondrial intracellular store in pancreatic acinar cells by inositol-1,4,5-trisphosphate. Nature 1983; 306: 67–9.

Timmerman LA, Clipstone NA, Ho SN, Northrop JP, Crabtree GR. Rapid shuttling of NF-AT in discrimination of Ca^{2+} signals and immunosuppression. Nature 1996; 383: 837–40.

Tran EH, Hoekstra K, Van Rooijen N, Dijkstra CD, Owens T. Immune invasion of the central nervous system parenchyma and experimental allergic encephalomyelitis, but not leukocyte extravasation from blood, are prevented in macrophage depleted mice. J Immunol 1998; 161: 3767–75.

Vig M, Peinelt C, Beck A, Koomoa DL, Rabah D, Koblan-Huberson M, et al. CRACM1 is a plasma membrane protein essential for store-operated Ca^{2+} entry. Science 2006; 312: 1220–3.

Weiner HL. Immunosuppressive treatment in multiple sclerosis. J Neurol Sci 2004; 223: 1–11.

Wekerle H, Kojima K, Lannes-Vieira J, Lassmann H, Linington C. Animal models. Ann Neurol 1994; 36: S47–53.

Yeromin AV, Zhang SL, Jiang W, Yu Y, Safrina O, Cahalan MD. Molecular identification of the CRAC channel by altered ion selectivity in a mutant of Orai. Nature 2006; 443: 226–9.